Geochemical Controls on the Uranium Cycle in a Lake Watershed

Pierre Lefebvre, Arnaud Mangeret, Alkiviadis Gourgiotis, Pascale Louvat, Pierre Le Pape, Pierre Sabatier, Olivier Diez, Charlotte Cazala, Jérôme Gaillardet, Guillaume Morin

Geochemical controls on the uranium cycle in a lake watershed

Pierre Lefebvre*[a,1], Arnaud Mangeret[b], Alkiviadis Gourgiotis[b], Pascale Louvat[c,2], Pierre Le Pape[a], Pierre Sabatier[d], Olivier Diez[b], Charlotte Cazala[b,3], Jérôme Gaillardet[c], Guillaume Morin[a]

a. *Institut de Minéralogie, de Physique des Matériaux et de Cosmochimie (IMPMC), UMR 7590 CNRS-Sorbonne Université-MNHN-IRD, 75252 Paris Cedex 05, France*

b. *Institut de Radioprotection et de Sûreté Nucléaire (IRSN), PSE-ENV SEDRE, 92262 Fontenay-aux-Roses Cedex, France*

c. *Université de Paris-Institut de Physique du Globe de Paris-CNRS, UMR 7154, 75238 Paris Cedex 05, France*

d. *Université Savoie Mont Blanc-CNRS, EDYTEM, UMR 5204, 73376 Le Bourget-Du-Lac Cedex, France*

New addresses:

1. Soil Chemistry Group, Institute of Biogeochemistry and Pollutant Dynamics, Department of Environmental Systems Science, ETH Zürich, 8092 Zürich, Switzerland

2. Université de Pau et des Pays de l'Adour, E2S UPPA, CNRS, IPREM, 64053 Pau Cedex 9, France

3. Université Paris Saclay, CEA, Service de physico-chimie, 91191 Gif-sur-Yvette Cedex, France

Accepted version

ACS Earth and Space Chemistry, 2023 – DOI: 10.1021/acsearthspacechem.2c00348

Virtual Special Issue "Environmental Redox Processes and Contaminant and Nutrient Dynamics"

*Corresponding author: Pierre Lefebvre, pierre.lefebvre @ usys.ethz.ch

ABSTRACT

Understanding the uranium (U) cycle – reservoirs and processes – at the watershed scale is key to manage contaminated areas, to elucidate ore formation processes as well as to implement paleoenvironmental research. Here, we investigated the different steps of the U cycle, from sources to sinks, and the relative roles of redox processes and organic matter in the control of U mobility in the naturally U-rich small mountainous watershed of Lake Nègre (France). We interpret the U repartition in U reservoirs through chemical, isotopic ($\delta^{238}U$ and ($^{234}U/^{238}U$)) and speciation analyses, in the light of anterior studies of the site. We show that U(VI) originates from the leaching of U-rich rock fractures and is transported in dissolved forms. Wetlands and meadow soils then act as intermediary sinks where U(VI) is complexed by organic matter (up to > 5000 µg/g) and subsequently partly reduced to U(IV). Dissolved U is also supplied to the lake, in addition to particulate and colloidal U resulting from soil physical erosion. After entering the lake, most U(VI)-bearing organic particles settle in the sediments and U(VI) is reduced to U(IV), resulting in high sedimentary U concentrations (up to > 1000 µg/g), while a fraction of U is potentially desorbed from particles. Remaining dissolved U is exported from the watershed through the lake outlet stream. In this high-mountain lake catchment, the U cycle is mainly controlled by organic matter complexation and particulate transport, though U reduction in the lake sediments may help to its long-term immobilization.

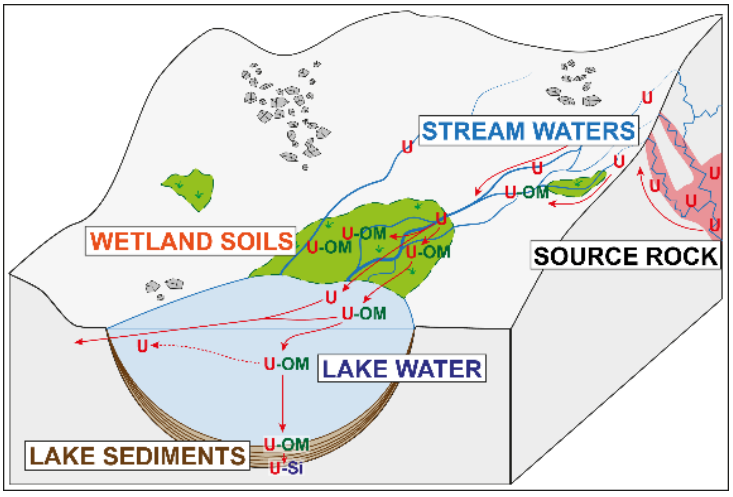

Keywords

Uranium speciation; Uranium isotopes; Lake watershed; Organic matter; Redox processes; Particulate transport

1. INTRODUCTION

Uranium (U) is a radionuclide naturally present at trace levels in the continental crust, with an average concentration estimated at 2.7 µg/g [1]. Nonetheless, high U accumulation in natural systems has been reported and is at the center of a variety of research fields. In addition to U mining for its use in the nuclear industry, and environmental studies on contaminated sites, it is also used in paleoenvironmental studies to assess the redox of ancient oceans through measurements of the U isotope ratios in sedimentary rocks [e.g., 2]. Understanding the U cycle in continental and marine systems is thus crucial to improve our knowledge of the mechanisms of U ore formation and U environmental contamination as well as the factors controlling U accumulation in sediments, including redox and particulate transport.

The uranium cycle has been assessed at the Earth's scale, particularly through investigation of the repartition of its isotopes in the different reservoirs [3,4]. Particular effort has been focused on the fate of U in oceans to constrain the controls on U scavenging in sediments to illuminate paleoredox studies [e.g., 5,4]. The main process of U removal from the oceans has been widely identified as U diffusion through the sediment-water interface followed by the reductive precipitation of dissolved U(VI) to solid-phase U(IV) [e.g., 6–8]. Besides extensive research on the U cycle in such large-scale systems, only a few studies have assessed the behavior of U in continental, freshwater systems. Beside studies on large river basins [e.g., 9,10], some research has been done on lacustrine systems, most of which focus on lake sediments and in some cases on the lake water column. A main interest of studying a lake watershed lies in the limited size of the system, which allows considering most of the U reservoirs and facilitates the determination of the processes at stake without major blind spots. Although freshwater differs in salinity from seawater, understanding the processes controlling the U cycle in a lake system, including its water column and sediments, can inform to a certain degree on redox and transport processes occurring in oceanic systems, with different space and time scales. In particular, mountainous lake catchments cover a reduced area, and U inputs to these catchments can be more easily constrained than in larger watersheds. A comprehensive assessment of the U cycle in such a well-constrained system could thus be achievable – although it still requires a high number of samples – and contribute to the understanding of the global U terrestrial cycle.

The previous studies on U in lake systems often described a specific process or reservoir of the U cycle, using either geochemical – including isotopic – proxies to reconstruct U sources and accumulation mechanisms [11–16] or spectroscopic tools to investigate the U oxidation state and

speciation in the lake sediments in order to track diagenetic processes [17,18]. The mode of U deposition in the sediments was shown to vary depending on the lake setting, either through authigenic U precipitation [14,15,17] or through settling of U-bearing organic or Fe/Mn-oxide particles [12,13,16] in addition to detrital inputs [12]. Some of these studies showed that oxidized U forms (U(VI)) can be released to pore water in oxygenated upper sediments [13], while U is reduced to less soluble U(IV) during anaerobic organic matter (OM) oxidation and Fe/Mn reduction in deeper layers [13,17]. However, to our knowledge, none of the previous works integrates the U cycle at the watershed scale, taking into account most sources and sinks and the main processes that control U mobility in a lake system. In particular, the respective roles of redox processes and transport with OM or Fe/Mn-oxide particles in driving U transfers are hard to decipher when using only one type of analytical tools.

In this study, we aimed to reconstruct the uranium cycle in the naturally U-rich small mountainous watershed of Lake Nègre (Mercantour-Argentera Massif, South-East France) by using a wide combination of samples (stream and lake waters, rocks, soils, and sediments) and analytical techniques. Lake Nègre is located 2354 m above sea level in a granitic area and was shown to contain exceptionally high U contents of natural origin, particularly in two types of reservoirs that are widely known to favor U accumulation: lake sediments and wetland soils. Our previous studies focused on the controls on U accumulation in the lake sediments over the past 9200 years [16], the mineralogical evolution of U species in the sediments [18], and the mechanisms leading to high U accumulation in soils of the wetland upstream of the lake [19]. In this work, we present new U concentrations and isotopic data from a variety of reservoirs in the watershed, including bedrock, soils and sediments, streams and lake column waters and interpret them in light of our previous studies on specific parts of the watershed. We focus our discussion on the geochemical processes controlling U mobility in the different reservoirs of the watershed, in order to reconstruct a qualitative U cycle in the Lake Nègre system, with only rough estimates of some U stocks and fluxes.

2. MATERIALS AND METHODS

2.1. Study site and sampling

2.1.1. The Lake Nègre watershed

The Lake Nègre watershed has been described in previous studies [16,18–20]. Briefly, this small glacier-carved catchment is located in the granitic Mercantour-Argentera Massif (Mediterranean Alps, South-East France) and is essentially covered by granite scree with disseminated alpine meadows and rare trees (Figure 1). The bedrock is mainly composed of leucogranite, partly milonitized south of the lake; a 10 m-wide lamprophyre dyke intrudes the granite NE of the lake [21]. The meadows are mainly found in the gentle slopes of the central part of the watershed (Figure 2). A few minerotrophic wetlands developed on flat areas; the main wetland (designated as ZH1) is situated on the northern (upstream) shore of Lake Nègre and was the subject of a detailed study [19]. Two low-flow creeks feed the lake: the eastern creek has its source in the scree NE of the lake and feeds a small pond (identified as PI2) before flowing down to wetland ZH1 by its east side (Figures 1 and 2); the western creek flows along a north-south axis and crosses an upper wetland (ZH2) before feeding the lake through the west side of ZH1 (Figure 2). At the time of our field sampling campaigns (September 2018, 2019, 2020 and 2021, see below), i.e., in summer with low rainfall, the western stream was flowing aboveground only over portions of the stream path (below ZH2), while the eastern stream was always flowing at the surface, in any case with a low flow rate.

The lake itself covers 10 hectares and has a 28 m deep water column which was shown to be stratified in September 2018, with a well-mixed upper layer (10 m) overlying a colder layer with lower – but significant – dissolved O_2 (ref 18). The lake sediments (> 2 m thick) have been deposited since the last deglaciation, prior to 11,200 Before Present (BP) [16]. They are organic-rich (gyttja-type) with low detrital contents [16,18].

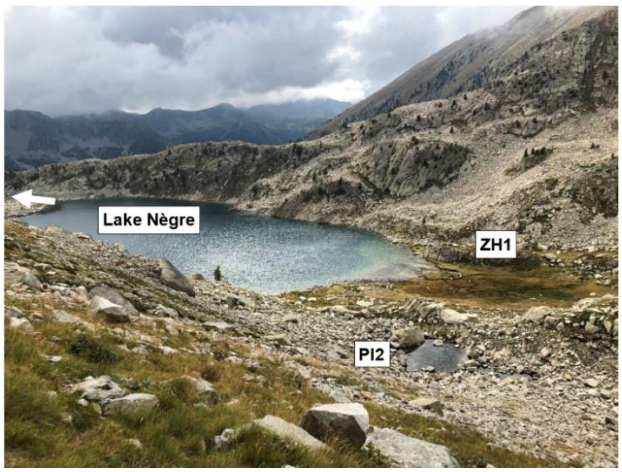

Figure 1 – Photograph of the southern part of the Lake Nègre watershed, taken from the northeast (see viewpoint in Figure 2). The spring of the eastern stream is located at the bottom right of the picture; the stream feeds a pond (PI2) before flowing to the lake through wetland ZH1. The lake outlet location and flow direction is indicated by a white arrow. The PI2 pond measures approximately 15 m in diameter and wetland ZH1 extends over ~80 m.

2.1.2. Sampling

Four field sampling campaigns in the Lake Nègre watershed took place in September 2018, 2019, 2020 and 2021. A variety of samples were collected to investigate the origin and fate of uranium in this exceptionally U-rich natural system. The locations of all samples described in this study are indicated in Figure 2. Photographs of most of the samples are shown in the *Supporting Information*. Additional descriptions of samples from this study and our previous works [16,18,19] with corresponding performed analyses are provided in a *Supplementary Data* file. During sampling and laboratory analyses, no unexpected or unusually high safety hazards were encountered.

A series of soils and surface sediments – in streambeds or on the shallow platform north of the lake – were sampled across the watershed (gray circles in Figure 2) and downstream of the lake outlet (EXU1). Two 30 cm soil cores – C1 and C2 – were taken in September 2018 in wetland ZH1 (black circles in Figure 2) and thoroughly characterized in ref 19. Two additional ZH1 soil cores were sampled in September 2021 for the present study: C1c (26 cm) at the location of core C1, and C4b (10 cm) in a puddle in which water was sampled (E4, bulk and 0.2 µm-filtered). A short (5 cm) core was collected in the small ZH5 dry wetland and divided into three slices.

A few samples of moss, algae and biofilms (grouped under the term “organic” in Figure 2) were also collected: floating algae in the PI2 pond, moss in the eastern stream (at point SCE1), moss and lichen in rock fractures presenting significant radioactivity, and biofilm up- and downstream of wetland ZH1.

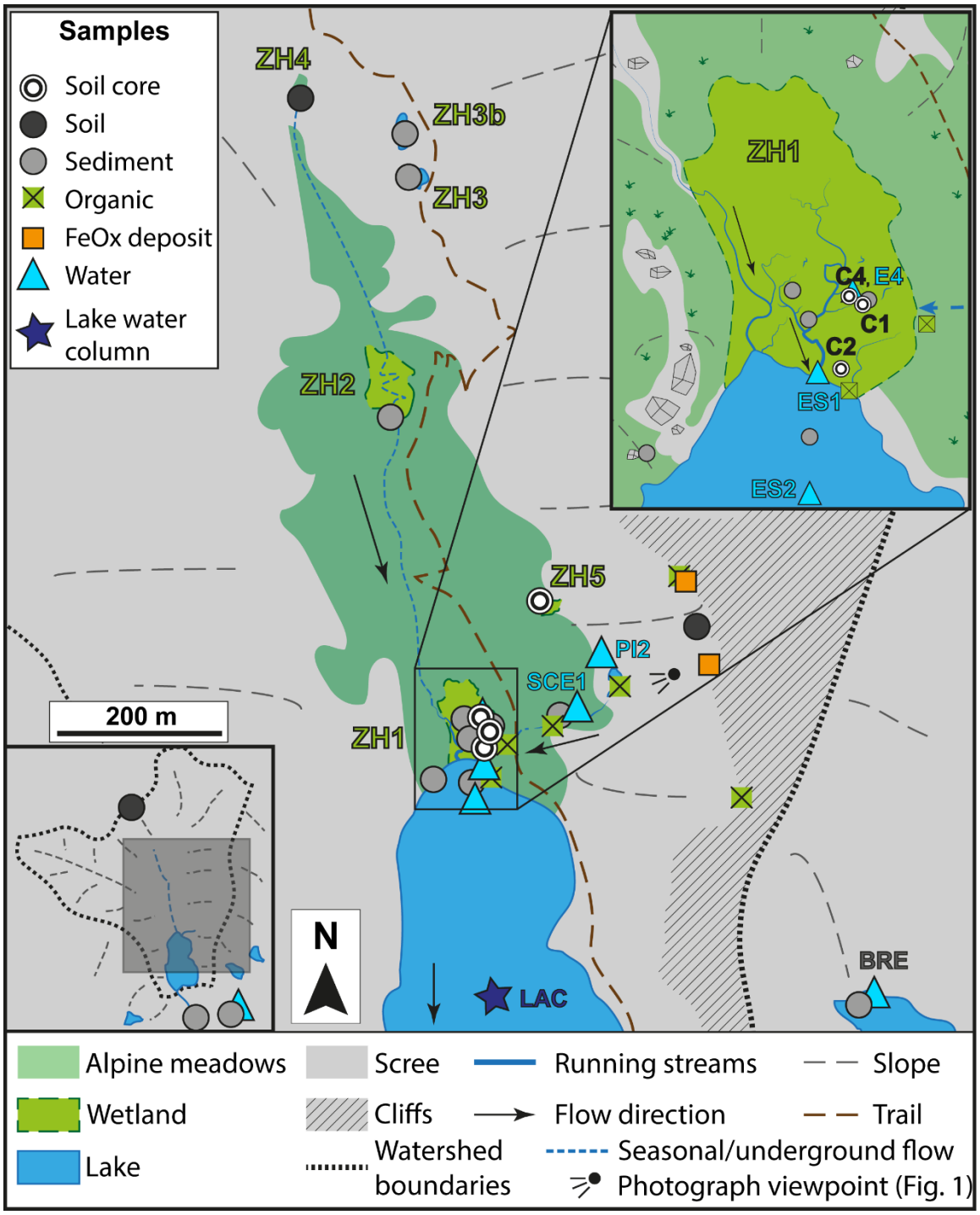

Figure 2 – Sampling locations on a simplified map of the southern part of the Lake Nègre watershed. Soils and sediments are represented by gray to black circles, organic samples (moss, algae, biofilms, lichen) by green crossed boxes and Fe oxides ("FeOx") deposits in rock fractures by orange squares. Waters sampling locations are shown by blue triangles with their respective labels, and the position of the lake water column sampling (LAC) is indicated by a blue star. The nomenclature of the main sampling zones (wetlands, seasonal ponds and large meadows – ZH1 to ZH5) is also indicated.

In September 2020, a radiologic survey of the bedrock was conducted with two probes: a Saphymo 6150 AD 6/H radiation meter coupled with a 6150 ADb probe for gamma dose rate measurements (in nanoSievert per hour, nSv/h) a few centimeters from the investigated rock and a NUVIATech CoMo 170 probe for alpha and beta count rates (in counts per second, cps) in contact with the rock. Rock samples were taken where the radioactivity was higher than the background gamma dose rate of ~250-300 nSv/h measured on most of the granite (with beta emission of approximately 50 counts per second (cps) and no measurable alpha emission). The highest count rates were detected in faults and fractures covered by iron oxides (see section 3.1.1). On two rock samples, the iron oxides ("FeOx deposits") were scratched with a geologist hammer for chemical analysis.

During the same field trip (in 2020), we sampled the lake water column as well as stream waters from the eastern creek that was previously shown to contain 2-3 times more U than the western creek [19]. The eastern stream samples were taken at the same locations as the previous study (in 2019): at the spring resurging from scree (PI2), upstream of the wetland (SCE1), at the wetland outlet (ES1) and 20 m downstream on a shallow platform north of the lake (ES2). The only difference is for the stream spring that was sampled 10 m downstream of the previous location (PI1), on the north side of the PI2 pond where the spring flows. The lake water column was sampled at the position of sediment core sampling [16,18] from an inflatable boat at six depths (0, 5, 10, 15, 20, 23 m) with an acid-cleaned Niskin bottle; because of windy conditions, the sampling positions are expected to be located within a 20-30 m diameter.

Throughout the whole procedure, acid-cleaned vials (HDPE bottles and centrifuge tubes) and filtration systems were used to avoid contamination. Immediately after sampling, the main physico-chemical parameters (pH, oxidation-reduction potential ORP, temperature, conductivity, dissolved O_2) were measured in unfiltered water samples with field WTW 350i and 3420 multi-parameter probes. The ORP was measured with a WTW Sentix ORP platinum-Ag/AgCl electrode. A series of (ultra-)filtration steps were performed on the water samples. First, an aliquot (500 mL) of the nonfiltered (bulk) water was taken; then 1.5 L were vacuum-filtered through a nitrocellulose 0.2 µm filter with an acid-cleaned Sartorius apparatus. Ultrafiltration was then performed with an Amicon cell under positive pressure, equipped with regenerated cellulose or PES (polyethersulfone) disks. All samples were ultrafiltered at 30 kDa immediately after the 0.2 µm filtration step. In addition, 7 samples were also filtered at 100 kDa and then at 30 kDa to evaluate the effect of the intermediate 100 kDa filtration on the final 30 kDa-filtered fractions. Forty milliliters from each filtered fraction were collected in a calcined brown glass vial for Dissolved Organic Carbon (DOC) measurements

(see Supporting Information); the remaining volume was collected in a plastic vial (bottle or tube). Here, the > 0.2 µm fraction is technically defined as "particulate", the size fraction between 0.2 µm and 30 kDa as "colloidal" and the < 30 kDa fraction as "truly dissolved".

Incidentally, no bulk (nonfiltered) sample was taken at point SCE1 before filtration. We thus collected a nonfiltered volume the next day and filtered an aliquot at 0.2 µm. Comparison of the two 0.2 µm-filtered samples collected one day apart showed a good agreement between U concentrations and U/Na ratios, indicating that the bulk sample can be properly compared with all filtered fractions taken one day before.

In addition to sampling in the Lake Nègre watershed, we investigated the watershed adjacent to Lake Nègre in the East (Figure S1) by collecting nonfiltered water and surficial sediments in two smaller lakes, Lac des Bresses (noted BRE, across the eastern ridge of the Lake Nègre watershed) and a shallow lake south of Lake Nègre (noted LACBIS), as well as suspended flocs from a large wetland at the outlet of this adjacent watershed (BRE-ZH1).

2.2. Chemical analyses

Most analytical procedures described here were fully detailed in our previous publications on Lake Nègre [16,18,19].

2.2.1. Organic matter characterization

The concentrations in light elements (C, H, N, S) associated to organic matter (OM) in soils and sediments were measured on precisely weighed aliquots at the LUTECE laboratory (IRSN) on a FlashSmart elemental analyzer (Thermo Scientific). C/N ratios were calculated as atomic (mol/mol) ratios.

2.2.2. Gamma spectrometry

Radionuclide activities (^{238}U (from ^{234}Th), ^{232}Th (from ^{228}Ac), ^{230}Th, ^{226}Ra, ^{210}Pb, ^{137}Cs, ^{40}K) were measured in soils and FeOx deposits by gamma spectrometry. The samples were dried in an oven at 30 °C, ground and resin-sealed in plastic vials for more than 3 weeks to allow the equilibration of radon isotopes (^{222}Rn and ^{220}Rn) with their parent and daughter radionuclides. Low quantities of Fe oxide deposits were homogenously diluted in silica powder to fit the detector efficiencies for each radionuclide of interest. We used a well-type high-purity/low-noise Ge ORTEC GWL Series detector, counting for 24 to 72 h depending on the sample radioactivity. Reference compounds RGU-1, RGTh-1, 131SL300 and 161SL300 (from IRSN) IAEA-312 and 314 (from IAEA) were also measured to

control the efficiency and background noise of the detectors. The gamma emission lines were identified and quantified with the Interwinner 5.0 software (ITECH Instruments). ^{238}U activities were obtained from ^{234}Th assuming secular equilibrium and converted to mass concentrations (µg/g) using the specific activity of 12.44 kBq/g.

2.2.3. Analysis of elemental concentrations

Concentrations of dissolved anions (F^-, Cl^-, Br^-, NO_2^-, NO_3^-, SO_4^{2-}) were determined in non-acidified waters aliquots filtered at 0.2 µm and 30 kDa using a 930 Compact IC Flex ionic chromatograph (Metrohm) at LUTECE. The results satisfyingly showed good agreement between both filtered fractions.

Major, minor and trace cations in waters and in some solids (organic samples and FeOx deposits) were analyzed by optical and mass spectrometry with a ThermoFisher ICAP 7600 DUO ICP-OES and an Agilent 8800 ICP-MS/MS at LUTECE. Prior to analysis, the organic samples (moss, algae, lichen, biofilms) were digested in acid-cleaned PTFE beakers with distilled (16 N) HNO_3 (heated at 90 °C) followed by $HClO_4$ addition (heated at 160 °C). Fe oxide samples were digested following a slightly different protocol, with a mix of 16 N HNO_3 and 27 N HF in the first step. Large volumes (100-750 mL) of non-filtered water samples were first evaporated and then digested in 16 N HNO_3. In a similar way, large volumes of the filtered waters (at 0.2 µm, 100 and 30 kDa) were evaporated and recovered in HNO_3 3 N.

2.2.4. Isotopic measurements

Uranium activity and isotopic ratios (($^{234}U/^{238}U$) and $^{238}U/^{235}U$, respectively) were determined in waters, in Fe oxides and in organic samples. Aliquots were double-spiked with the IRMM3636 standard solution (with a spike/sample $^{236}U/^{235}U$ ratio of 3) and U was separated on a UTEVA resin column (Eichrom Technologies). The isotopic measurements were performed on a Neptune MC-ICP-MS (Thermo Finnigan) at the PARI platform (IPGP), using Faraday cups equipped with feedback resistors of 10^{11} Ω (for $^{233, 235, 236, 238}U^+$ and ^{232}Th isotopes) and 10^{13} Ω (for $^{234}U^+$ isotope and the $^{239}Pu^+$ for the estimation of $^{238}UH^+$ formation). The sample measurements were bracketed with standard IRMM-184, and sample $^{235}U/^{238}U$ ratios were converted to the delta notation ($\delta^{238}U$) relative to the bracketing standard measured ratios. The provided $\delta^{238}U$ values were eventually expressed relative to the commonly used standard CRM-145. ($^{234}U/^{238}U$) activity ratios were obtained by multiplying the corresponding isotopic ratio with the ratio of radioactive decay constants. The measurements accuracy was verified by analyzing reference materials HU-1 and BCR-2 that were prepared

following the same procedure as for samples. The uncertainties were calculated as two standard deviations (2SD) of 3 to 5 replicate measurements of each sample.

The isotopic ratios were measured in bulk, 0.2 µm- and 30 kDa-filtered fractions of the stream and lake waters and found to be equal within uncertainties (Figure S2). Consequently, we chose to average all three measurements (bulk, 0.2 µm- and 30 kDa-filtered) for each water sample.

Additionally, ($^{234}U/^{238}U$) activity ratios were measured on six surface soil samples following UTEVA resin separation, using an Agilent 8800 ICP-MS/MS at LUTECE. The measurements accuracy was verified by analyzing reference materials HU-1 and IRMM-184. The uncertainties were calculated as 2SD based on 3 replicate measurements of each sample.

2.2.5. Electron microscopy

A few rock samples from radioactive fractures were investigated by Scanning Electron Microscopy on a Zeiss Ultra 55 microscope equipped with a Field Emission Gun and an Energy-dispersive X-ray spectrometer (SEM-EDX) at the IMPMC platform. The rock samples were first cut with a diamond wire saw and polished before being metalized with carbon. SEM-EDX investigation was conducted in backscattered electron mode (AsB) at a working distance of 7.5 mm with a 15 kV emission. The EDX spectra were calibrated using the Cu K_α emission line of Cu tape.

3. RESULTS AND DISCUSSION

3.1. Uranium sources and preferential pathways

3.1.1. Uranium source rock

In previous field campaigns, we sampled rocks across the watershed which low U concentrations (2-6 µg/g, ref 18) could presumably not account for the high U accumulation in the wetland soils and in the lake sediments (up to > 5000 µg/g and > 1000 µg/g respectively [18,19]). The above-mentioned discovery of faults and fractures with significant radioactivity shed light on the unanswered question of the original U source. Although the radiological survey did not homogenously cover the entire watershed, it appears from our measurements that the count rates were higher on the eastern side of the watershed (Figure 3). The faults and fractures showing the highest count rates often display quartz veins and are covered by iron oxides that may also be present at depth and not only at the rock surface. A significant gamma dose rate was detected (up to 950 nSv/h) along with beta (up to 150 cps) and alpha (up to 2.7 cps) counts, the latter being putatively attributed to the presence of U. These features may correspond either to (i) recent deposits where circulating groundwater resurges at the surface and is exposed to oxygen and/or to (ii) older mineralization from hydrothermal processes during the granite metamorphism, oxidized upon exhumation. Anecdotally, the lamprophyre dyke (spessartite-type) intruding the granite north of the lake was found to be even less radioactive than the granite (gamma dose rate 200 nSv/h, beta emission 40 cps, no alpha emission) and is thus likely not a source of U.

A microscopic investigation of rock samples by SEM-EDX revealed the occurrence of trace U in thin Fe oxide veins widely distributed across the rock (Figure S3). Some of these microscopic veins seem to originate from cubic-shaped iron oxide minerals (Figure 4), some of which are zoned and contain trace S (Figure S4). Such a pattern suggests that these cubic-shaped minerals may have been pyrite (FeS_2) grains oxidized to Fe oxides by a circulating fluid (either hydrothermal or supergene). This observation would be consistent with past reducing conditions where pyrite would have precipitated from hydrothermal fluids. These conditions are also known to be favorable to the reductive precipitation of U(IV) minerals (uraninite UO_2 or coffinite $USiO_4$, for instance) [e.g., 22,23]. Upon oxidation, iron sulfides may have formed iron (oxyhydr)oxides that could have scavenged U(VI) by adsorption [e.g., 24–26]. Additionally, we found traces of U in (possibly organic) concretions on aluminosilicate crystals (Figure S5), which may be due to secondary precipitation or adsorption.

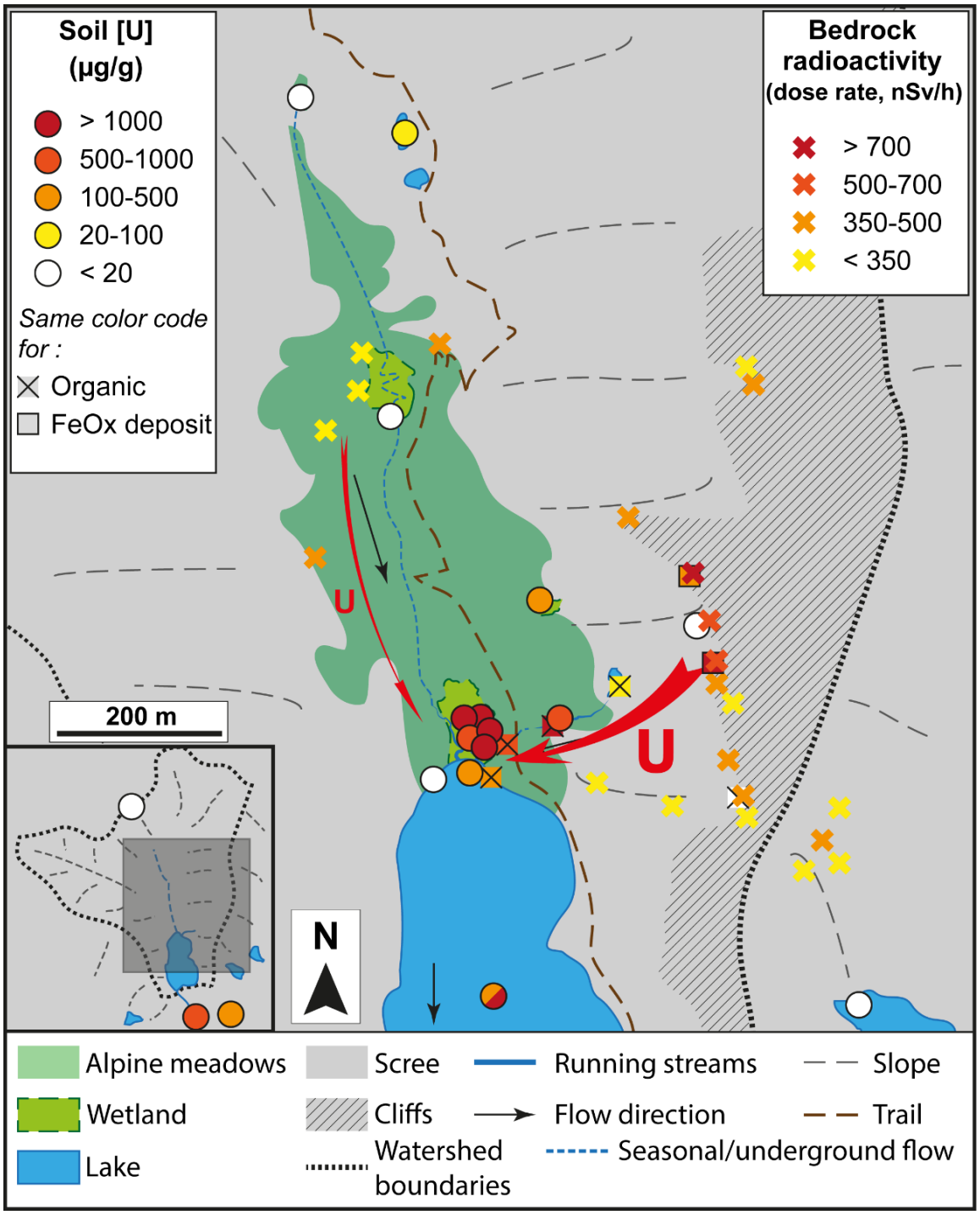

Figure 3 – Geographical distribution of uranium contents in rocks, soils and sediments of the Lake Nègre watershed. Measurements of the bedrock radioactivity (gamma dose rate, in nSv/h) are indicated by crosses; U concentrations (µg/g) in surface soils and sediments are indicated by circles, in organic samples (moss, algae, biofilms) by crossed boxes and in Fe oxide deposits by squares. Highest U/radioactivity levels are represented in dark red, low U/radioactivity in yellow to white.

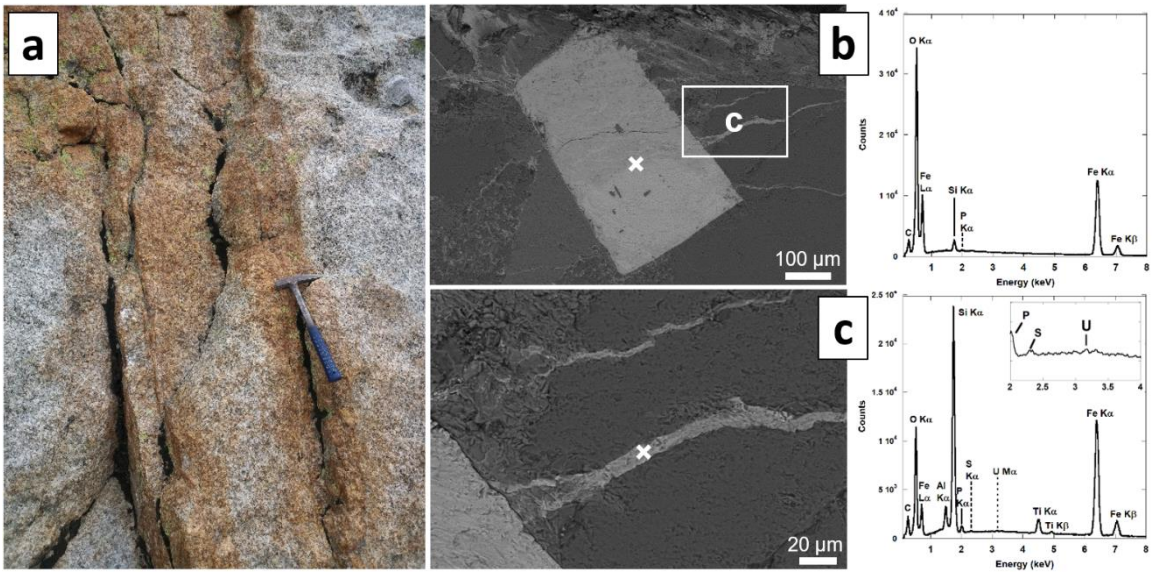

Figure 4 – (a) Photograph of a Fe oxides-covered fault with radioactivity above the background (gamma dose rate 950 nSv/h, beta emission 150 cps, alpha emission 2.3 cps); (b) SEM micrograph of cubic-shaped Fe oxide with the associated EDX spectrum (taken at the white cross position) from the same rock; (c) Fe oxide microscopic fracture extending from (b) with its EDX spectrum showing traces of U (see inset).

Another clue to the origin of U in the Lake Nègre system is provided by the activities of ^{238}U daughter radionuclides ^{234}U, ^{230}Th and ^{226}Ra. These radionuclides were measured in three samples of Fe oxide deposits scratched from two rocks with high count rates (see *Supplementary Dataset*). The oxides were found to contain from 161 to 1115 µg/g U (^{238}U activities between 2007 ± 470 and 13870 ± 780 Bq/kg), that is likely of non-detrital origin as ^{228}Ac activities (indicative of ^{232}Th, classically used as a proxy of the bedrock detrital component) are very low (36-332 Bq/kg). The Fe oxide deposits display (^{234}U/^{238}U) activity ratios above secular equilibrium with values of 1.171 ± 0.007 and 1.130 ± 0.005 (Figure 5), in contrast to the bulk granite that was found to be at secular equilibrium [18]. These high activity ratios indicate that U found in the fractures is relatively recent, i.e., younger than ~2.5 million years (required to reach secular equilibrium). This U deposition thus cannot be linked to the Hercynian emplacement and later Alpine deformation of the bedrock Argentera granite (respectively ~300 and 22 My [e.g., 27]). Note that the exhumation of the analyzed fractures probably occurred through glacier carving during the last glacial period (i.e., maximum 115 ky). The ^{234}U-enrichment process in the fracture Fe oxides is likely due to preferential leaching of ^{234}U because of alpha recoil [e.g., 28] that was further transported and accumulated in the fractures [e.g., 29]. The variability of (^{234}U/^{238}U) ratios may be attributed to variable

chemical erosion rates of the primary U source [30] and/or to variable ages of U deposition in the fractures.

In the analyzed U-rich Fe oxide deposits, high ^{230}Th activities (7113 ± 4160 to 20731 ± 6226 Bq/kg) were recorded, that are superior or at least equal (considering uncertainties) to ^{238}U and ^{234}U activities. This observation likely suggests that a fraction of U has been lost from the fractures. Additionally, (^{226}Ra/^{238}U) activity ratios range from 0.89 ± 0.7 to 2.4 ± 0.7, corresponding to (^{226}Ra/^{230}Th) values between 0.34 ± 0.11 and 0.60 ± 0.10. These results indicate either that ^{226}Ra is not equilibrated yet with its parent or more likely that a fraction of Ra was lost as well. These observations resemble those made on soil samples from the wetland ZH1 in our anterior study, where U and Ra were found to be mobile [19].

Overall, these arguments support the hypothesis that U is supplied to the Lake Nègre watershed from the chemical erosion of the bedrock, likely by supergene processes, i.e., by the circulation of meteoric water in the fractures that dissolves U and transports it to the surface and subsequently to the creeks (probably in U(VI) forms). On its path, U may be transiently scavenged through adsorption on Fe oxides and later remobilized. With the available data, we could not precisely determine the primary origin of fracture-deposited U, which may originate either from the leaching of deep U-rich fractures and/or from large-scale leaching of the bulk granite.

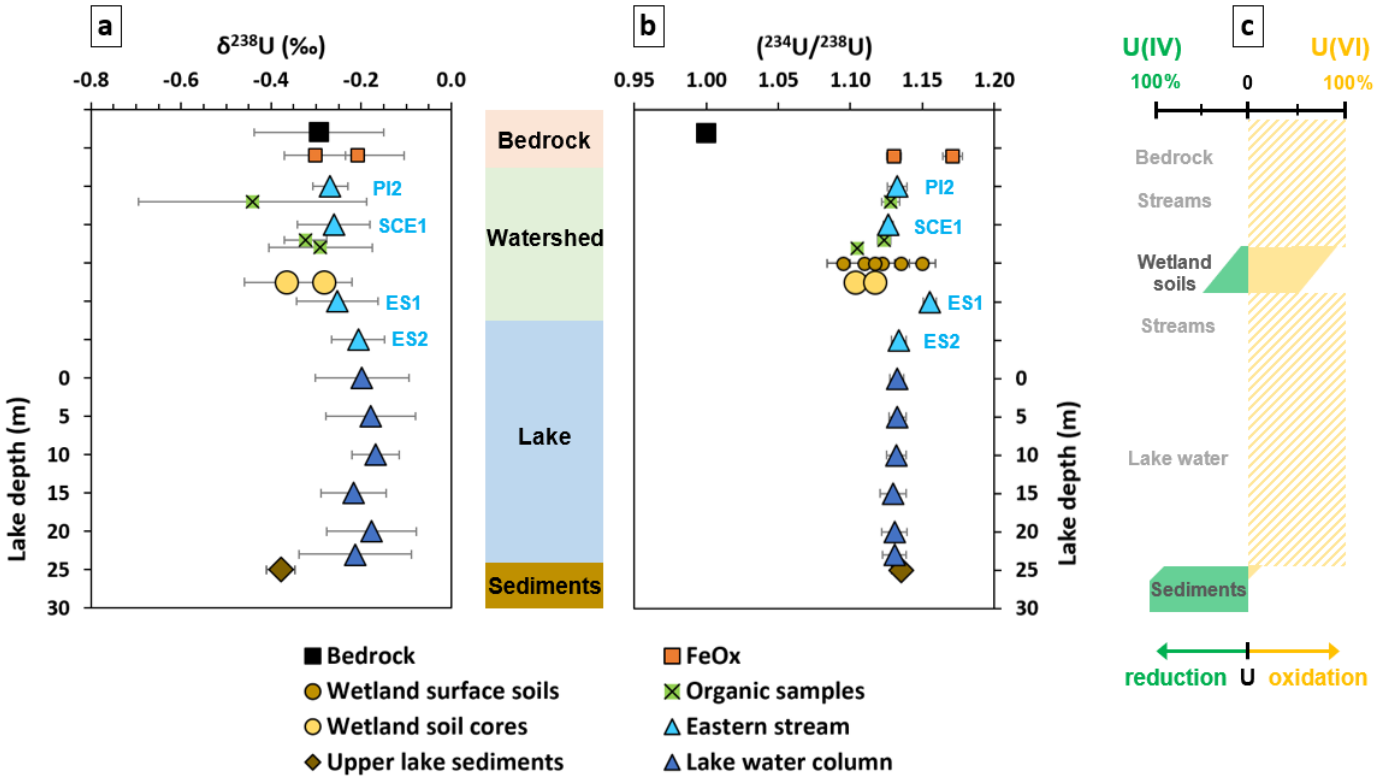

Figure 5 – Uranium isotopic signatures (a) $\delta^{238}U$ and (b) ($^{234}U/^{238}U$) and (c) estimated U oxidation state from samples of the Lake Nègre watershed along a vertical downstream gradient. (a-b) The granitic bedrock is represented by a black square, Fe oxides ("FeOx") deposits in rock fractures by orange squares, stream waters by light blue triangles (with sample names), organic samples (moss, algae, biofilm) by green crossed boxes, surface soils from wetland ZH1 by light brown circles, soil cores from wetland ZH1 (average values) by yellow circles, lake water column samples at different depths by dark blue triangles and upper lake sediments (Unit T) by a brown diamond. The most downstream water sample from the eastern stream (ES2, lowest light blue triangle) is located at the lake inlet. (c) U(IV) and U(VI) proportions in U reservoirs are represented in green and orange, respectively. The U oxidation state was measured in previous studies [18,19] by U L_3-edge X-Ray Absorption Near-Edge Structure (XANES) spectroscopy in the wetland soils (between 46 and 90 % U(VI), average 74 % (ref 19)) and in the lake sediments (from 16 % U(VI) in the upper sediments to 0 % in the deeper sediments [18]). In the other compartments (Fe oxide deposits, creek and lake waters; dashed areas), U is expected to be mostly in U(VI) forms. Error bars represent 2SD uncertainties.

3.1.2. Geographical distribution of U accumulation in the Lake Nègre watershed

The heterogeneous distribution of U concentrations in soils and sediments across the watershed is in line with the location of U source rocks (Figure 3) [31]. The highest U concentrations – up to > 1000 µg/g in surface sediments and even > 5000 µg/g in soil cores of ZH1 [19] – are found mainly on the eastern side of the watershed, downstream of the U-bearing rocks and on the path of the eastern

stream. This is consistent with higher dissolved U in the eastern stream than in the western one, as recorded in our previous study [19]. These observations may however be subject to a potential sampling bias, as the eastern side was more investigated than the western side of the watershed.

Biological objects (moss, algae, biofilm) were also found to scavenge high amounts of U: floating algae in the PI2 pond accumulated 75 µg/g U (dry weight), and biofilms in wetland ZH1 contain 141 to 511 µg/g U. The highest U content was measured in moss collected in the eastern stream at point SCE1 (upstream of wetland ZH1), with a 1795 µg/g U accumulation in this plant. The exception is for lichen sampled in a moderately radioactive fracture, which contains only 5.2 µg/g U.

In summary, the geographical distribution of U accumulation in the Lake Nègre watershed indicates that U originates from U-rich hydrothermal veins located on the east side and exposed to supergene chemical weathering and erosion. Uranium is then transported by surface stream waters to the downstream meadows and wetlands and ultimately to the lake.

3.1.3. Uranium accumulation in the adjacent watershed

Variable but overall lower U contents were found in surface sediments and waters sampled in the watershed easterly adjacent to Lake Nègre (Figure S1). Background U concentrations were measured in the small Lake des Bresses east of Lake Nègre, with only 8 µg/g in the sediment and 0.016 µg/L in the lake water. Higher U amounts were found in the sediments of a small lake southeast of Lake Nègre (143-217 µg/g), which water contains 2.7 µg/L of U, as well as in the suspended flocs of the wetland located at the outlet of this adjacent watershed (162-295 µg/g). This confirms the presence of some U sources in the mountain ridge east of Lake Nègre, but also indicates that the exceptional U enrichments in the Lake Nègre watershed are caused by local processes.

3.2. Uranium transport and accumulation in soils of the watershed

3.2.1. Uranium transport in stream waters

At the time of sampling in September 2020, the stream waters had dissolved O_2 levels close to equilibrium with the atmosphere (6.6-8.1 mg/L), oxidation-reduction potentials in the 200-250 mV range, and low conductivity values typical of mountainous streams (20-98 µS/cm) (see *Supplementary Dataset*). The pH values ranged between 6.95 and 8.81 and were higher or equal to that of our previous field campaign in September 2019 (ref 19) as shown in Table S1. In the lake water column, the conductivity was also low (22-42 µS/cm), ORP was measured between 182 and 245 mV, and dissolved O_2 decreased with depth (from 6.7 mg/L at the surface to 3.9 mg/L at 23 m

depth). The measured pH also showed a decreasing trend from 9.28 at the surface to 6.73 at depth (Table S1).

Comparison of the water samples filtered at 30 kDa with or without the intermediate 100 kDa filtration step showed that this additional filtration retained on average 14 % of U. As a consequence, the colloidal fraction (between 0.2 µm and 30 kDa) was overestimated in this case. We therefore chose to present filtration results with the only two consecutive filtration steps at 0.2 µm and 30 kDa, which were performed on all 10 water samples.

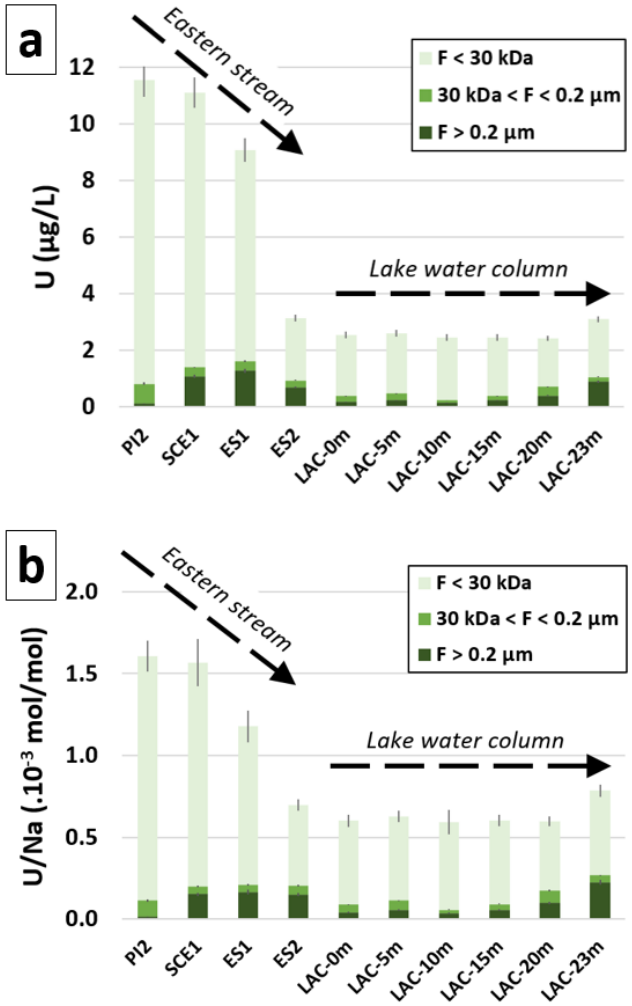

Figure 6 – Uranium repartition in particulate (> 0.2 µm), colloidal (30 kDa < F < 0.2 µm) and truly dissolved fractions (< 30 kDa) of waters sampled in the eastern stream and in the lake, as U concentrations (a) and U/Na molar ratios (b). U concentrations were normalized by invariant Na to account for dilution. PI2 is the spring of the eastern stream feeding the wetland through SCE1, before flowing into the lake at ES1, diluted 20 m further at ES2. The Lake Nègre water column was sampled in the central part of the lake at six depths: 0, 5, 10, 15, 20 and 23 m. The sampling locations are illustrated in Figures 1 and 2. Error bars represent 2 SD uncertainties.

Overall, uranium concentrations and isotopic compositions of stream waters sampled at the same locations one year apart (in September 2019 (ref 19) and 2020) were found to be highly comparable (Figure S6). The main difference lies in the proportion of U in the colloidal fraction, which was likely overestimated in our previous study because of intermediary filtration steps [19].

After being dissolved from U-rich source rocks, U is transported downstream by ground- and runoff waters, likely in U(VI) forms, with U concentrations of 9.1-11.6 µg/L in the eastern creek and 2.4-3.1 µg/L in the lake (Figure 6). In water sampled at the spring of the eastern stream (PI2) and slightly downstream (SCE1), the ($^{234}U/^{238}U$) activity ratio is disequilibrated with values around 1.13 (Figure 5b). Uranium is present mostly in the truly dissolved fraction (< 30 kDa), although the U proportion bound to suspended particles significantly increases between PI2 and SCE1 (Figure 6). It should be noted that chemical erosion of U from the source rock does not seem to cause any significant isotopic fractionation, as attested by similar $\delta^{238}U$ signatures between the rock and the stream water (Figure 5a). This observation is in line with several studies, although there is no consensus on the potential isotopic fractionation associated to chemical erosion [see the review by 32].

3.2.2. Uranium scavenging through complexation by soil organic matter

One of our previous studies [19] specifically investigated the mechanism of U scavenging in the soils of wetland ZH1 over thousand years and showed that the primary process was U complexation (sorption) to a variety of organic particles with variable affinity to U. This was demonstrated through a combination of geochemical, isotopic, microscopic and spectroscopic techniques. In particular, we used U L_3-edge X-ray Absorption Spectroscopy (XAS) to show that dissolved U(VI) first accumulates in mononuclear forms by dominant monodentate binding to organic C moieties and is then partly reduced to U(IV) (Figure 5c) [19]. U was found to be dispersed on a variety of organic particles with variable local U accumulation (up to 3 at%), but with a homogenous oxidation state at the sample scale. Although the impact of seasonal soil redox cycling (due to variations in the water table depth and snow cover) on U redox and mobility is difficult to estimate with discrete sampling, it appears that the main parameter driving U accumulation in the wetland soils is complexation to OM followed by a limited reduction of U(VI) to U(IV) rather than reduction of U(VI) to U(IV) followed by authigenic U(IV) precipitation.

Here, the identification of U sorption by OM in the wetland soils as the dominant U scavenging mechanism [19] is again confirmed by little to no isotopic fractionation between the wetland inlet water (SCE1) and the soil cores of the wetland (Figure 5a). Indeed, U adsorption is generally expected to result in a slight – if any – enrichment of the light isotopes in the solid phase, while U

reduction favors heavy isotopes in the reduced solid-phase U(IV) [see the review by 32]. This pattern is also observable in algae, moss and biofilm, which therefore also accumulate U through sorption.

Along the upper stream section (between PI2 and SCE1) and after crossing the wetland (between SCE1 and ES1), we observe a slight decrease in the stream water U concentration and U/Na ratio that cannot be explained by dilution (Figure 6), as also observed in 2019 (ref 19). This result further attests the impact of U scavenging in the meadows and wetland soils on U transfers along the stream course.

3.2.3. Organic matter in soils and sediments

The organic matter content (represented by TOC) of soils and sediments across the watershed is highly variable, with values ranging from 0.4 to 41.1 wt% (Figure S7). The highest TOC values are recorded in soil core C2 of wetland ZH1 (ref 19), where soils are more developed and accumulated more detrital OM than the scarce meadows upstream of the watershed, where TOC rarely exceeds 10 wt%. This variability in OM contents, in conjunction with different U supplies depending on the geographical position, may explain the variability in U accumulations across the watershed (Figure 3). In this line, U/TOC ratios also show considerable variations from 0.2 to 61 mg_U/g_{TOC} (Figure 7), with an average value of 13.9 mg_U/g_{TOC} and a median of 8.4 mg_U/g_{TOC} (n = 26).

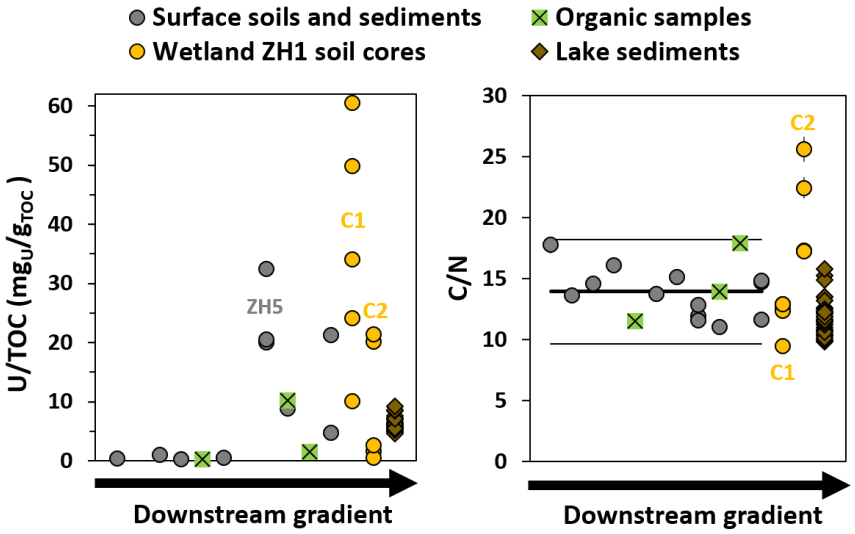

Figure 7 – Distribution of (left) U/TOC mass ratios and (right) C/N atomic ratios along a downstream gradient in soils and sediments of the Lake Nègre watershed, from the watershed heights to the lake sediments. Surface soils and sediments are represented by gray diamonds, organic samples (moss, algae, biofilm) by green crossed boxes, soil samples from cores C1 and C2 in wetland ZH1 by yellow circles (C1: left, C2: right) and sediments from core NEG18-06 [16] by brown circles. The average C/N value of surface soils and sediments and organic samples (13.9 ± 4.3) is shown by a thick black line, with 2SD intervals indicated by thin black lines. Error bars represent 2 SD uncertainties.

C/N atomic ratios can be used to identify the origin and type of OM [33], which plays a major role in the U cycle. The C/N ratios of organic matter across the watershed upstream of wetland ZH1 are rather homogenous and have an average value of 13.9 ± 4.3 (Figure 7). In the soil cores of ZH1, the diverging C/N values between the two cores C1 and C2 may be explained by the depositional environment. Core C1 was taken under stagnant water and is rich in diatoms, which are expected to have lower C/N ratios [33]. Core C2 was taken in a seasonally dry streambed and consists mainly of organic-rich soils that are thought to be composed of old vegetal remains from vascular plants – with high C/N (ref 33) – that developed earlier in the watershed [16].

The measured average C/N in the present-day watershed soils is in good agreement with the "meadow-type" environment C/N endmember described in our paleo-environmental study on Lake Nègre sediments [16]. In this anterior study, the meadow C/N was assumed to lie between 13 and 20 and was even constrained in a mixing model to be between 13 and 14, which is exactly in the range obtained here.

3.3. Uranium transport to the lake

3.3.1. Particulate and dissolved U transfers

Although U concentrations in the creek slightly decrease along the stream path, a concomitant increase in the proportion of U borne by suspended particles (> 0.2 µm) is observed (Figures 6 and S8). As in our previous study [19], we could not precisely determine the water DOC content in filtered fractions and thus cannot confirm the nature of U-bearing particles. However, considering that U predominantly accumulates on organic matter in wetland soils [19], it is plausible that U-bearing suspended particles in streams and in the lake are mostly organic. This likely indicates that U is exported from the watershed soils through the physical erosion of U-bearing organic matter. This interpretation is further attested by the observation of a significant correlation between terrigenous OM and U fluxes to the lake sediments over the last 7000 years [16]. However, one should keep in mind that in such a scenario, the U export from soils to the lake sediments through erosion dominantly occurs during high precipitation events. Low-flow periods such as that at the time of sampling most likely account for a minor fraction of the U export budget to the lake sediments. Nevertheless, some observations on the U-involving processes occurring at the time of sampling in the streams and in the lake can still be drawn with the available data. In particular, lake water is expected to be buffered and less subject to short-term variations than stream water.

When reaching the lake at point ES2, the eastern stream is readily diluted with U concentrations divided by three (Figure 6), as observed in 2019 (ref 19). The U concentration in the lake appears to be rather homogenous at approximately 2.5-3 µg/L, on the shore and along the water column at the center of the lake (Figure 6a). However, a significant U increase is observed in the deepest sample (23 meters, at 1-2 m above the sediment at this location), which is linked to a higher U fraction borne by suspended particles (29 % of total U) (Figure S8). We exclude a sampling bias such as resuspension of the sediment by the Niskin bottle. Indeed, the sampled water was visually limpid, and such a bias would likely have resulted in a much higher amount of particulate U, as the upper sediment contains ~350 µg/g U (ref 18). The increasing particulate U concentration in deep lake waters is likely attributed to slight natural sediment resuspension in the benthic boundary layer [e.g., 34], rather than upward diffusion from the upper sediments, as U concentrations are slightly lower in the pore waters [18].

Overall, on its path from the source rocks to the lake, U is first under dissolved forms, then partially scavenged into the soils and further exported with organic particles and colloids through soil erosion down to the lake. In low-flow periods, a major proportion of U is still dissolved in the streams and in the lake, but we suppose that U fluxes in particulate and colloidal forms are higher during heavy rain events. Incidentally, the low proportion of U bound to colloids and particles likely explains the absence of resolvable difference in $\delta^{238}U$ isotopic signatures between the filtered fractions (bulk, 0.2 µm- and 30 kDa-filtered) of all water samples (Figure S2).

3.3.2. Isotopic insights into U sources and transport mechanism

Interestingly, variable ($^{234}U/^{238}U$) activity ratios were measured in the wetland soils (1.095 ± 0.011 to 1.150 ± 0.009), with values often below that of the wetland inlet (1.132 ± 0.007 and 1.126 ± 0.003) and outlet waters (1.155 ± 0.005) as well as the upper lake sediments (1.135 ± 0.007) (Figure 5b). In particular, the core soils are depleted in ^{234}U compared to most samples from the watershed, with average ($^{234}U/^{238}U$) of 1.104 ± 0.001 and 1.117 ± 0.003 for cores C1 and C2, respectively [19]. The most likely explanation to this observation is that spatial and temporal variability in the chemical erosion rate of the bedrock can induce variations in the ($^{234}U/^{238}U$) signature of dissolved U [30,35,36]. Hence, the ($^{234}U/^{238}U$) signatures in the wetland soils and in the stream waters would record the variability of the U sources ($^{234}U/^{238}U$) both in space (e.g., potential underground water flow feeding different parts of the wetland in addition to creeks [31]) and in time (e.g., seasonal variations of weathering and erosion intensity, long-term changes in the creek paths) [37]. In this regard, because they integrate most of U fluxes downstream of the watershed and because

of their relative homogeneity, the lake water column and lake sediments would display the average ($^{234}U/^{238}U$) signature of the watershed.

For soils that have been accumulating U for several thousand years (such as the deeper layers of the wetland soil cores [19]), we cannot exclude an additional mechanism of preferential ^{234}U mobility leading to lower ($^{234}U/^{238}U$) ratios. As discussed in ref 19, this mechanism could be preferential leaching of ^{234}U from wetland soils because of alpha recoil effects, either through direct ^{234}Th recoil into pore water or through damage to the U binding site [e.g., 38]. This preferential diffusion of ^{234}U has been observed for instance in marine organic-rich sediments [39]. With such a phenomenon, the older soil layers would be progressively depleted in ^{234}U over thousand years. However, this mechanism alone cannot explain the difference in ($^{234}U/^{238}U$) between the soils and the sediments and would therefore be complementary of the U source variability described above.

Additionally, the importance of precipitation events in the sedimentary U budget is highlighted by the discrepancy between the stream and lake water $\delta^{238}U$ signatures and that of the recently deposited sediments which is ~0.2 ‰ lower and more comparable to the wetland soil $\delta^{238}U$ (Figure 5a). Two hypotheses may explain such a fractionation. First, U could accumulate in the sediments through diffusion at the sediment-water interface and sorption to sedimentary OM (not by reductive precipitation, excluded in light of the sediment $\delta^{238}U$ value that should be much higher in this case [5,40,41]). Second, the analyzed lake water could be non-representative of the global U inputs to the sediments; this would be the case if most U was supplied as particle-bound U during high precipitation events. The first hypothesis is expected to be unlikely, as the lake U concentrations may not be able to account for such high sedimentary U. For example, U accumulation in the euxinic Black Sea sediments that are very favorable to U scavenging leads to U concentrations generally < 20 µg/g with a seawater U of 1.5-2 µg/L [e.g., 40] and a comparable sediment accumulation rate [42]. In comparison, reaching 350 µg/g of sedimentary U from an oxic water column at 2.5-3 µg/L in Lake Nègre appears highly improbable. The second hypothesis is much more plausible considering the discussion above. In this scenario, most uranium in the lake water column at the time of sampling would not be directly linked to (i.e., precursor of) sedimentary U. The measured lake water U concentrations at such a "steady state" would thus result from a balance between dissolved U inputs from streams, dilution by rainwater and potential desorption from U-bearing settling particles. The latter phenomenon is plausible considering the change in the water physico-chemical conditions (notably pH, rising from acidic to circumneutral values – 5.5 to 7 – in the wetland to ~9 in the lake; Table S1) and is compatible with the measured $\delta^{238}U$, with dissolved U isotopically heavier than particulate – i.e., sedimentary – U (Figure 5a).

3.4. Uranium export from the lake water

As a consequence of the discussions above, two main processes of U export from the lake water occur simultaneously, which relative importance in terms of quantitative U fluxes cannot be determined with the available data: U accumulation in the lake sediments and U export through the lake outlet.

As stated above, U accumulation in Lake Nègre sediments is controlled by the settling of U-rich organic particles originating from erosion of the U-scavenging watershed soils. This is supported by the U solid-state speciation in the upper lake sediments determined in a previous study [18], where U was shown to be in noncrystalline forms and bound to organic carbon and silica (abundant because of diatom frustules). This accumulation process has been occurring for 7000 years, with a potentially different mechanism prior to 7000 years before present [16]. Anterior characterization of the sedimentary organic matter indicated that terrigenous OM (in contrast to autochthonous OM) was responsible for U inputs to the lake over this period [16], in line with the interpretations of the present study. The increasing contribution of autochthonous OM to the sedimentary OM budget over the last 3500 years only resulted in dilution of the sedimentary U content [16] and lower U/TOC ratios in the sediments compared to the soils (Figure 7).

Although it is expected that U is oxidized in the water column (U(VI) sorbed on settling organic particles), sedimentary U was found in a previous study to be mostly reduced even in the upper 1.5 centimeters (84 ± 3 % of U(IV)) [18]. This indicates that reducing conditions are readily established in the sedimentary column, in accordance with the absence of dissolved oxygen in the pore waters below 2 mm (ref 18). At depth in the sediments, all U is reduced to U(IV) within uncertainties (Figure 5c). After deposition and over at least 3300 years, the U speciation was shown to transform upon diagenesis in the lake sediments, forming U-Si polymers in less than 700 years, with a local structure resembling that of coffinite $USiO_4$ (ref 18). Such a result indicates that reducing conditions have likely persisted over several thousand years in the deep sediments of the lake, which may have contributed to long term immobilization of U, in addition to complexation processes.

In this regard, the redox conditions of the lake sediments – permanently reducing – are unsurprisingly radically different from those of the wetland soils – predominantly oxidizing, with expected seasonal redox cycling. However, higher U contents were found in the wetland soils than in the lake sediments despite this difference (up to 5200 and 1250 µg /g respectively [16,19]; Figure 3).

This finding highlights the predominance of terrestrial organic matter in controlling U mobility in the Lake Nègre watershed, both as a U scavenger in the soils and as a vector of U transport through erosion, rather than U redox as expected with the common paradigm linking U accumulation to its reduction.

Uranium export through the lake outlet is attested by the measurement of U concentration in the outlet stream (2.3 ± 0.1 µg/L (refs 18, 19)) which is only slightly inferior to that of the lake. This observation is confirmed by a high U concentration of 828 µg/g measured in surface sediments collected in the outlet stream ~400 m downstream of the lake (Figure 3).

3.5. Estimation of uranium stocks and flux to the sediments

Although an accurate quantification of U stocks and fluxes in the Lake Nègre watershed is not achievable with the available data, a few rough estimations can be drawn to obtain orders of magnitude. In particular, we calculated approximate U stocks in the wetland soils, in the lake sediments and in the lake water column, and the current U flux from the lake water column to the sediments.

The lake volume was modeled as a semiellipsoid (Figure S9), using approximate lake dimensions of 500 x 240 m, with a maximum water depth of 28 m (ref 20). The total lake water volume is therefore of ~1.8 x10^6 m^3. Considering an average U concentration of 2.5 µg/L (Figure 6), the total U mass in the Lake Nègre water column was on the order of 4 kg at the time of sampling.

The total volume of lacustrine sediments was estimated with the same ellipsoid model, using a maximum sediment depth of 1 m (Figure S9). The latter value was evaluated considering only pristine sedimentary units T and B described in refs 16 and 18 and extrapolating the sediment accumulation rate to the estimated maximum age of the lake, corresponding to the last deglaciation ~13.000-14.500 years before present [43]. The sediment volume is therefore ~ 6.3 x10^4 m^3, corresponding to ~1.3 x10^7 kg of sediments with an average dry bulk density of 0.21 g/cm^3 (ref 16). Uranium contents in the sediments probably depend on the distance to the wetland and are variable with depth, covering a range from 350 to 1200 µg/g in the cores sampled at the deepest point of the lake, in a position close to the lake center; we therefore chose a median value of 780 µg/g (from high-resolution U measurements on sediment cores [16]) as the order of magnitude of sedimentary U. With these values, the U stock in Lake Nègre sediments is roughly estimated at ca. 1 x10^4 kg.

The current and past fluxes of U to the lake sediments could also be assessed using the sediment accumulation rate, the sediment dry bulk density (DBD) and the sediment U content (which could be spatially heterogeneous, see previous paragraph). In the upper sediments deposited over the past 50 years, the sediment accumulation rate was measured at 0.69 mm/yr (ref 18) and the DBD at 0.33 g/cm^3. This corresponds to approximately 14 tons of sediments depositing each year at the bottom of the lake, with a U content of 350 µg/g (ref 18), i.e., ~5 kg of U accumulating annually in the Lake Nègre sediments during the past 50 years. The U fluxes were lower over the past 9200 years: for example, at 7000 years BP, the accumulation rate was 0.064 mm/yr and the DBD 0.17 g/cm^3, with a U content of 1100 µg/g (ref 16), corresponding to approximately 0.7 tons of sediment and ca. 0.8 kg of U depositing each year at that time. More generally, these past U fluxes to the lake sediments were estimated with a high time resolution between 9200 and 50 yr BP in ref 16, with an average U flux per unit area of 10.7 ± 3.0 mg/m^2/yr. These fluxes were shown [16] to be one to two orders of magnitude higher than the fluxes to marine sediments in the Black Sea [6] and the California margin [8] for example. Considering the approximate surface of the lake bottom (~10.2 ha), this would be equivalent to roughly 1.1 ± 0.3 kg of U per year over most of the Holocene. The 5-fold increase in U fluxes to the sediments in recent years is likely due to a significant increase in physical erosion rates over the last century, even higher than the increase recorded over the last 1600 years [16].

We eventually evaluated the order of magnitude of the U stock in the soils of wetland ZH1 upstream of the lake. The wetland volume was modeled as a cuboid with dimensions of 80x50 m and an approximate depth of 50 cm (the soils cores sampled in depressions measured 30 cm down to the granitic sand [19]). The dry bulk density could not be measured and was considered equivalent to that of the lake sediments, i.e., ~0.2 g/cm^3. Again, the soil U content is highly variable, spanning a range of 100-5200 µg/g depending on the distance to U sources [31]. We chose an order of magnitude of 1500 µg/g (median of 38 soil measurements from this study and ref 19), resulting in a roughly estimated U stock in the wetland soils of ~ 600 kg.

Although these numbers should be interpreted with caution, a few general insights may be drawn from these orders of magnitude. Because of major volume differences, the lake sediments are the main U reservoir in the lake watershed, rather than the wetland soils, although the latter display locally higher U contents. Additionally, the amount of U that accumulates every year in the lake sediments (U bound to OM particles from the watershed soils) is on the same order of magnitude as the total U stock in the lake water column at the time of sampling, i.e., in a period of low particulate transport. The amount of U transiting each year through the lake column water to the sediments

(mostly during high precipitation events) is therefore comparable to the U amount contained in the "steady-state" lake water. Finally, because we do not know the water discharge at the lake outlet, it is impossible to determine which U export flux is most important between the outlet stream and the lake sediments.

4. CONCLUSIONS

In the present study, we characterized a variety of U-rich reservoirs in the Lake Nègre watershed in order to establish an overview of the U cycle in this system, in the light of our previous publications detailing U accumulation and evolution in the lake sediments and the wetland soils. In summary, the main processes controlling the uranium cycle in the Lake Nègre watershed can be described as shown in Figure 8, from source (1) to sinks (3 and 6/6'):

1) Uranium originates from the leaching of the bedrock by ground- and meteoric waters; in particular, U-rich fractures, which may have been formed by ancient hydrothermal and/or recent supergene processes, may be the main U sources to the watershed;
2) Dissolved U is transported by streams, mainly from the east side of the Lake Nègre watershed;
3) In the watershed meadows and in wetland ZH1 right upstream of Lake Nègre, dissolved U (in U(VI) forms) is scavenged through complexation by soil organic matter and partly reduced to U(IV); the highest U accumulations in the watershed (several thousand μg/g in noncrystalline forms) are recorded in the wetland;
4) While U is continuously supplied to the lake in dissolved forms, most of the U transferred to the lake sediments comes from the physical erosion of soil U-rich organic particles;
5) These U-rich particles then sink down to the lake sediments; 5') a fraction of U might be desorbed from organic particles, resulting in additional dissolved U;
6) In the sediments, organic-bound noncrystalline U progressively evolves to form U-Si polymers under persisting reducing conditions in a Si-rich medium; 6') Dissolved U is exported through the lake outlet stream.

A major result of this study is that U mobility in the Lake Nègre watershed is controlled by organic matter through complexation and further export by particulate and colloidal transport. In particular, redox processes seem to have a minor impact on U mobility in the watershed soils and in the lake sediments, in contrast to many other systems described in the literature.

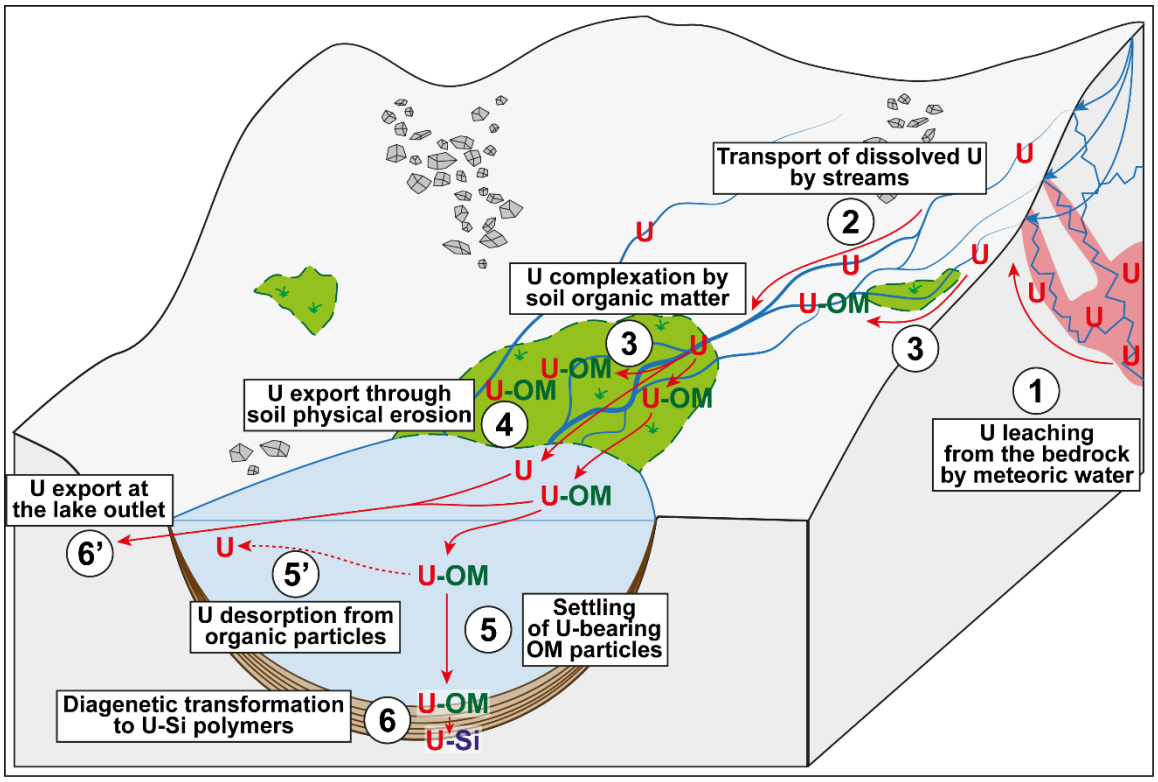

Figure 8 – Simplified conceptual model of the U cycle in the Lake Nègre watershed, from source (1) to sinks (3 and 6/6'). Uranium paths are represented in red. "U" indicates dissolved U, "U-OM" is for uranium bound to organic matter, and "U-Si" for uranium-silica polymers in aged sediments.

The exceptional U accumulation in the Lake Nègre watershed appears to be caused by local conditions, which may be either (i) a particular U source that supplies high U amounts and/or (ii) more efficient U scavenging processes in the Lake Nègre wetland than in comparable wetland systems. We showed that the watershed bedrock likely supplies high U amounts thanks to ancient hydrothermal vein U enrichment. The second condition would imply that wetland ZH1 has original features that are particularly favorable to U accumulation, for example a type of organic matter with very high affinity to U, or specific geochemical parameters (such as low dissolved inorganic carbon, pH, redox). Identifying the key parameter responsible for such original U enrichments would require further investigation including a comparison with other alpine wetlands.

The present study focused on the current U cycle in the Lake Nègre watershed, with a few insights on its temporal evolution enabled by studying the lake sedimentary archives. In particular, increasing erosion rates over the past 50 year caused a 5-fold increase in the flux of U to the lake sediments. The future evolution of the lake watershed with regard to climate change – for example

with increasing vegetation cover [e.g., 44] – may impact even more the U cycle, through changes in erosion rates and in the amount of U scavenged by OM in the watershed soils.

Acknowledgments

The authors are grateful to Mathilde Zebracki, Pascale Blanchart, Didier Jézéquel, Fériel Skouri-Panet, Emmanuel Malet and Jean-Louis Reyss for their help in field sampling and Cyrielle Jardin, Lucas Nouveau, Gilles Alcalde and Imène Estève for their help in laboratory analyses. This study was realized with the approval of the Director of the Parc National du Mercantour. We greatly acknowledge the Parc National and Marie-France Leccia for enabling access to and sampling in the Lake Nègre watershed. This study was supported by IRSN through collaborative research program n° LS 20942 and by the Programme National EC2CO-BIOHEFECT/ECODYN (PUMA). Parts of this work were supported by IPGP multidisciplinary program PARI and by Paris–IdF Region SESAME Grant no. 12015908. This study contributes to the IdEx Université de Paris ANR-18-IDEX-0001. This is PATERSON, the IRSN's mass spectrometry platform, contribution no. 18. The authors wish to thank the Guest Editors, the Editor Prof. Joel D. Blum and two anonymous reviewers for their constructive comments that significantly improved this manuscript strength and clarity.

Supporting Information: Photographs of samples, additional data (U concentration and isotopic data, SEM micrographs and EDX spectra) (DOCX file). List of samples: description and analyses (DOCX file). Research data tables (XLSX file).

REFERENCES

(1) Rudnick, R. L.; Gao, S. Composition of the Continental Crust. In *The crust*; Treatise on Geochemistry; Elsevier, 2003; Vol. 3, pp 1–64.
(2) Lau, K. V.; Romaniello, S. J.; Zhang, F. *The Uranium Isotope Paleoredox Proxy*; Elements in Geochemical Tracers in Earth System Science; Cambridge University Press, 2019. https://doi.org/10.1017/9781108584142.
(3) Tissot, F. L. H.; Dauphas, N. Uranium Isotopic Compositions of the Crust and Ocean: Age Corrections, U Budget and Global Extent of Modern Anoxia. *Geochimica et Cosmochimica Acta* **2015**, *167*, 113–143. https://doi.org/10.1016/j.gca.2015.06.034.
(4) Andersen, M. B.; Vance, D.; Morford, J. L.; Bura-Nakić, E.; Breitenbach, S. F. M.; Och, L. Closing in on the Marine 238U/235U Budget. *Chemical Geology* **2016**, *420*, 11–22. https://doi.org/10.1016/j.chemgeo.2015.10.041.
(5) Andersen, M. B.; Romaniello, S.; Vance, D.; Little, S. H.; Herdman, R.; Lyons, T. W. A Modern Framework for the Interpretation of 238U/235U in Studies of Ancient Ocean Redox. *Earth and Planetary Science Letters* **2014**, *400*, 184–194. https://doi.org/10.1016/j.epsl.2014.05.051.
(6) Anderson, R. F.; Fleisher, M. Q.; LeHuray, A. P. Concentration, Oxidation State, and Particulate Flux of Uranium in the Black Sea. *Geochimica et Cosmochimica Acta* **1989**, *53* (9), 2215–2224. https://doi.org/10.1016/0016-7037(89)90345-1.
(7) Klinkhammer, G. P.; Palmer, M. R. Uranium in the Oceans: Where It Goes and Why. *Geochimica et Cosmochimica Acta* **1991**, *55* (7), 1799–1806. https://doi.org/10.1016/0016-7037(91)90024-Y.
(8) McManus, J.; Berelson, W. M.; Klinkhammer, G. P.; Hammond, D. E.; Holm, C. Authigenic Uranium: Relationship to Oxygen Penetration Depth and Organic Carbon Rain. *Geochimica et Cosmochimica Acta* **2005**, *69* (1), 95–108. https://doi.org/10.1016/j.gca.2004.06.023.
(9) Palmer, M. R.; Edmond, J. M. Uranium in River Water. *Geochimica et Cosmochimica Acta* **1993**, *57* (20), 4947–4955. https://doi.org/10.1016/0016-7037(93)90131-F.
(10) Charbonnier, Q.; Clarkson, M. O.; Hilton, R. G.; Vance, D. Source versus Weathering Processes as Controls on the Mackenzie River Uranium Isotope Signature. *Chemical Geology* **2023**, *625*, 121409. https://doi.org/10.1016/j.chemgeo.2023.121409.
(11) Edgington, D. N.; Robbins, J. A.; Colman, S. M.; Orlandini, K. A.; Gustin, M.-P. Uranium-Series Disequilibrium, Sedimentation, Diatom Frustules, and Paleoclimate Change in Lake Baikal. *Earth and Planetary Science Letters* **1996**, *142* (1), 29–42. https://doi.org/10.1016/0012-821X(96)00085-4.
(12) Chappaz, A.; Gobeil, C.; Tessier, A. Controls on Uranium Distribution in Lake Sediments. *Geochimica et Cosmochimica Acta* **2010**, *74* (1), 203–214. https://doi.org/10.1016/j.gca.2009.09.026.
(13) Och, L. M.; Müller, B.; März, C.; Wichser, A.; Vologina, E. G.; Sturm, M. Elevated Uranium Concentrations in Lake Baikal Sediments: Burial and Early Diagenesis. *Chemical Geology* **2016**, *441*, 92–105. https://doi.org/10.1016/j.chemgeo.2016.08.001.
(14) Dang, D. H.; Wang, W.; Pelletier, P.; Poulain, A. J.; Evans, R. D. Uranium Dispersion from U Tailings and Mechanisms Leading to U Accumulation in Sediments: Insights from Biogeochemical and Isotopic Approaches. *Science of The Total Environment* **2018**, *610–611*, 880–891. https://doi.org/10.1016/j.scitotenv.2017.08.156.
(15) Wang, W.; Dang, D. H.; Novotnik, B.; Phan, T. T.; Evans, R. D. Variations in U Concentrations and Isotope Signatures in Two Canadian Lakes Impacted by U Mining: A Combination of Anthropogenic and Biogeochemical Processes. *Chemical Geology* **2019**, *506*, 58–67. https://doi.org/10.1016/j.chemgeo.2018.12.029.
(16) Lefebvre, P.; Sabatier, P.; Mangeret, A.; Gourgiotis, A.; Le Pape, P.; Develle, A.-L.; Louvat, P.; Diez, O.; Reyss, J.-L.; Gaillardet, J.; Cazala, C.; Morin, G. Climate-Driven Fluxes of Organic-Bound

Uranium to an Alpine Lake over the Holocene. *Science of The Total Environment* **2021**, *783*, 146878. https://doi.org/10.1016/j.scitotenv.2021.146878.
(17) Stetten, L.; Mangeret, A.; Brest, J.; Seder-Colomina, M.; Le Pape, P.; Ikogou, M.; Zeyen, N.; Thouvenot, A.; Julien, A.; Alcalde, G.; Reyss, J. L.; Bombled, B.; Rabouille, C.; Olivi, L.; Proux, O.; Cazala, C.; Morin, G. Geochemical Control on the Reduction of U(VI) to Mononuclear U(IV) Species in Lacustrine Sediments. *Geochimica et Cosmochimica Acta* **2018**, *222*, 171–186. https://doi.org/10.1016/j.gca.2017.10.026.
(18) Lefebvre, P.; Gourgiotis, A.; Mangeret, A.; Sabatier, P.; Le Pape, P.; Diez, O.; Louvat, P.; Menguy, N.; Merrot, P.; Baya, C.; Zebracki, M.; Blanchart, P.; Malet, E.; Jézéquel, D.; Reyss, J.-L.; Bargar, J. R.; Gaillardet, J.; Cazala, C.; Morin, G. Diagenetic Formation of Uranium-Silica Polymers in Lake Sediments over 3,300 Years. *PNAS* **2021**, *118* (4), e2021844118. https://doi.org/10.1073/pnas.2021844118.
(19) Lefebvre, P.; Le Pape, P.; Mangeret, A.; Gourgiotis, A.; Sabatier, P.; Louvat, P.; Diez, O.; Mathon, O.; Hunault, M. O. J. Y.; Baya, C.; Darricau, L.; Cazala, C.; Bargar, J. R.; Gaillardet, J.; Morin, G. Uranium Sorption to Organic Matter and Long-Term Accumulation in a Pristine Alpine Wetland. *Geochimica et Cosmochimica Acta* **2022**, *338*, 322–346. https://doi.org/10.1016/j.gca.2022.10.018.
(20) AERMC. *Etude paléolimnologique sur 8 lacs du district Rhône-Méditerranée. Mise en place d'éléments de référence pour les lacs des 9 Couleurs, d'Anterne, de Chalain, de Lauvitel, Nègre, de Remoray, du Vallon et de Vens 1er, Années 2007-2008*; 3112EAFB08; Agence de l'eau Rhône, Méditerranée et Corse, 2008.
(21) BRGM. Carte Géologique Détaillée de La France [921-947], Saint-Martin-Vésubie – Le Boréon, 1967.
(22) Robertson, J. A. *The Blind River Uranium Deposits: The Ores and Their Setting*; Canada, 1976; p 45.
(23) Li, L.; Wang, Z.; Xu, D. Relationship between Uranium Minerals and Pyrite and Its Genetic Significance in the Mianhuakeng Deposit, Northern Guangdong Province. *Minerals* **2021**, *11* (1), 73. https://doi.org/10.3390/min11010073.
(24) Gallegos, T. J.; Fuller, C. C.; Webb, S. M.; Betterton, W. Uranium(VI) Interactions with Mackinawite in the Presence and Absence of Bicarbonate and Oxygen. *Environ. Sci. Technol.* **2013**, *47* (13), 7357–7364. https://doi.org/10.1021/es400450z.
(25) Othmane, G.; Allard, T.; Morin, G.; Sélo, M.; Brest, J.; Llorens, I.; Chen, N.; Bargar, J. R.; Fayek, M.; Calas, G. Uranium Association with Iron-Bearing Phases in Mill Tailings from Gunnar, Canada. *Environ. Sci. Technol.* **2013**, *47* (22), 12695–12702. https://doi.org/10.1021/es401437y.
(26) Lahrouch, F.; Guo, N.; Hunault, M. O. J. Y.; Solari, P. L.; Descostes, M.; Gerard, M. Uranium Retention on Iron Oxyhydroxides in Post-Mining Environmental Conditions. *Chemosphere* **2021**, *264*, 128473. https://doi.org/10.1016/j.chemosphere.2020.128473.
(27) Corsini, M.; Ruffet, G.; Caby, R. Alpine and Late-Hercynian Geochronological Constraints in the Argentera Massif (Western Alps). *Eclogae geol. Helv.* **2004**, *97* (1), 3–15. https://doi.org/10.1007/s00015-004-1107-8.
(28) Kigoshi, K. Alpha-Recoil Thorium-234: Dissolution into Water and the Uranium-234/Uranium-238 Disequilibrium in Nature. *Science* **1971**, *173* (3991), 47–48. https://doi.org/10.1126/science.173.3991.47.
(29) Smellie, J. A. T.; Mackenzie, A. B.; Scott, R. D. An Analogue Validation Study of Natural Radionuclide Migration in Crystalline Rocks Using Uranium-Series Disequilibrium Studies. *Chemical Geology* **1986**, *55* (3), 233–254. https://doi.org/10.1016/0009-2541(86)90027-6.
(30) Andersen, M. B.; Erel, Y.; Bourdon, B. Experimental Evidence for 234U–238U Fractionation during Granite Weathering with Implications for 234U/238U in Natural Waters. *Geochim Cosmochim Acta* **2009**, *73* (14), 4124–4141. https://doi.org/10.1016/j.gca.2009.04.020.

(31) Schumann, R. R.; Zielinski, R. A.; Otton, J. K.; Pantea, M. P.; Orem, W. H. Uranium Delivery and Uptake in a Montane Wetland, North-Central Colorado, USA. *Applied Geochemistry* **2017**, *78*, 363–379. https://doi.org/10.1016/j.apgeochem.2017.01.001.
(32) Andersen, M. B.; Stirling, C. H.; Weyer, S. Uranium Isotope Fractionation. *Rev Mineral Geochem* **2017**, *82* (1), 799–850. https://doi.org/10.2138/rmg.2017.82.19.
(33) Meyers, P. A.; Teranes, J. L. Sediment Organic Matter. In *Tracking Environmental Change Using Lake Sediments: Physical and Geochemical Methods*; Last, W. M., Smol, J. P., Eds.; Developments in Paleoenvironmental Research; Springer Netherlands: Dordrecht, 2001; Vol. 2, pp 239–269. https://doi.org/10.1007/0-306-47670-3_9.
(34) Boudreau, B. P.; Jorgensen, B. B. *The Benthic Boundary Layer: Transport Processes and Biogeochemistry*; Oxford University Press, 2001.
(35) Li, L.; Chen, J.; Chen, T.; Chen, Y.; Hedding, D. W.; Li, G.; Li, L.; Li, T.; Robinson, L. F.; West, A. J.; Wu, W.; You, C.-F.; Zhao, L.; Li, G. Weathering Dynamics Reflected by the Response of Riverine Uranium Isotope Disequilibrium to Changes in Denudation Rate. *Earth and Planetary Science Letters* **2018**, *500*, 136–144. https://doi.org/10.1016/j.epsl.2018.08.008.
(36) Thollon, M.; Bayon, G.; Toucanne, S.; Trinquier, A.; Germain, Y.; Dosseto, A. The Distribution of (234U/238U) Activity Ratios in River Sediments. *Geochimica et Cosmochimica Acta* **2020**, *290*, 216–234. https://doi.org/10.1016/j.gca.2020.09.007.
(37) Riotte, J.; Chabaux, F. (234U/238U) Activity Ratios in Freshwaters as Tracers of Hydrological Processes: The Strengbach Watershed (Vosges, France). *Geochimica et Cosmochimica Acta* **1999**, *63* (9), 1263–1275. https://doi.org/10.1016/S0016-7037(99)00009-5.
(38) Chabaux, F.; Riotte, J.; Dequincey, O. U-Th-Ra Fractionation During Weathering and River Transport. *Rev Mineral Geochem* **2003**, *52* (1), 533–576. https://doi.org/10.2113/0520533.
(39) Gourgiotis, A.; Reyss, J.-L.; Frank, N.; Guihou, A.; Anagnostou, C. Uranium and Radium Diffusion in Organic-Rich Sediments (Sapropels). *Geochemistry, Geophysics, Geosystems* **2011**, *12* (9). https://doi.org/10.1029/2011GC003646.
(40) Rolison, J. M.; Stirling, C. H.; Middag, R.; Rijkenberg, M. J. A. Uranium Stable Isotope Fractionation in the Black Sea: Modern Calibration of the 238U/235U Paleo-Redox Proxy. *Geochimica et Cosmochimica Acta* **2017**, *203*, 69–88. https://doi.org/10.1016/j.gca.2016.12.014.
(41) Brüske, A.; Weyer, S.; Zhao, M.-Y.; Planavsky, N. J.; Wegwerth, A.; Neubert, N.; Dellwig, O.; Lau, K. V.; Lyons, T. W. Correlated Molybdenum and Uranium Isotope Signatures in Modern Anoxic Sediments: Implications for Their Use as Paleo-Redox Proxy. *Geochimica et Cosmochimica Acta* **2020**, *270*, 449–474. https://doi.org/10.1016/j.gca.2019.11.031.
(42) Glenn, C. R.; Arthur, M. A. Sedimentary and Geochemical Indicators of Productivity and Oxygen Contents in Modern and Ancient Basins: The Holocene Black Sea as the "Type" Anoxic Basin. *Chemical Geology* **1985**, *48* (1), 325–354. https://doi.org/10.1016/0009-2541(85)90057-9.
(43) Brisset, E.; Guiter, F.; Miramont, C.; Revel, M.; Anthony, E. J.; Delhon, C.; Arnaud, F.; Malet, E.; de Beaulieu, J.-L. Lateglacial/Holocene Environmental Changes in the Mediterranean Alps Inferred from Lacustrine Sediments. *Quaternary Science Reviews* **2015**, *110*, 49–71. https://doi.org/10.1016/j.quascirev.2014.12.004.
(44) Carlson, B. Z.; Corona, M. C.; Dentant, C.; Bonet, R.; Thuiller, W.; Choler, P. Observed Long-Term Greening of Alpine Vegetation—a Case Study in the French Alps. *Environ. Res. Lett.* **2017**, *12* (11), 114006. https://doi.org/10.1088/1748-9326/aa84bd.